BN nanospheres as CpG ODN carriers for activation of toll-like receptor 9

Chunyi Zhi,[*a] Wenjun Meng,[bc] Tomohiko Yamazaki,[bc] Yoshio Bando,[a] Dmitri Golberg,[a] Chengchun Tang[a] and Nobutaka Hanagata[*bcd]

[a]International Center for Materials Nanoarchitectonics (MANA), National Institute for Materials Science (NIMS), Namiki 1-1, Tsukuba, Ibaraki, 305-0044, Japan
[b]Graduate School of Life Science, Hokkaido University, N10W8, Kita-ku, Sapporo, 060-0812, Japan
cBiomaterials Center, National Institute for Materials Science (NIMS), 1-2-1 Sengen, Tsukuba, Ibaraki, 305-0047, Japan
[d]Nanotechnology Innovation Center, National Institute for Materials Science (NIMS), 1-2-1 Sengen, Tsukuba, Ibaraki, 305-0047, Japan

Corresponding Authors:
Chunyi Zhi, ZHI.Chunyi@nims.go.jp
Nobutaka Hanagata, HANAGATA.Nobutaka@nims.go.jp

For the first time, we demonstrated BN nanospheres (BNNSs) can interact with biomolecules and deliver unmethylated cytosine-phosphate-guanine oligodeoxynucleotides (CpG ODNs) into cells to activate toll-like receptor 9 (TLR9), which is a very important process for therapy of cancers and allergy diseases.

Hexagonal boron nitride (h-BN) has attracted more and more attention due to its novel properties and structural similarity with carbon materials. Benefiting from a layered structure, it can form various morphologies, including tubes,[1] spheres,[2,3] sheets,[4–6] etc. In most cases, in spite of different morphologies, all structures of h-BN possess constant and wide band gaps, excellent mechanical properties, superb thermal conductivity, etc.[7] Recently, good biocompatibility was revealed for BNnanomaterials.[8,9] As far as bio-applications are concerned, spheres are considered to be more suitable than other morphologies due to advantages such as lower fibrous structure induced toxicity, easier cell uptake, etc.[10,11] Unmethylated cytosine-phosphate-guanine oligodeoxynucleotides (CpG ODNs) can be recognized by toll-like receptor 9 (TLR9), one of the innate immune receptors of the toll-like family.[12,13] The interaction between CpG ODN and TLR9 transduces an intracytoplasmic activation signal to activate NF-kB and subsequently induces

secretion of Th1-type cytokines and chemokines.[14] The resulting Th1-type immune response is essential for the therapy of cancers and allergies. However, application of the unmodified natural CpG ODN with a phosphodiester backbone to immunotherapy has been notably limited by its extreme susceptibility to nuclease degradation which renders it inactive in the free form.[15] Recently, increasing effort has been made to use various particles as delivery vehicles, such as liposomes and biodegradable microparticles, to codeliver CpG ODN with antigens as well as protect it against enzymatic degradation.[16–20] However, many delivery systems are involved in modified CpG ODN, which may cause toxic effects.[21,22] Therefore, it remains a challenge to develop suitable delivery systems for natural CpG ODN.

In this paper, highly pure BN nanospheres (BNNSs) were synthesized and adopted for delivering CpG ODN into cells for activation of TLR9. The interaction of BNNSs and deoxyribonucleic acid (DNA) was firstly investigated and it was revealed that DNA can be absorbed on BNNSs and released at controlled conditions. Moreover, it was demonstrated that BNNSs can easily be taken into cells and located in the lysosome compartments. Finally, BNNSs were used as carriers of CpG ODN to activate TLR9, and the results indicate that natural phosphorodiester CpG ODN loaded BNNSs exhibited significantly higher NF-kB activity compared with free CpG ODNs and pristine BNNSs.

BNNSs were synthesized by a chemical vapor deposition reaction between B(OMe)3 and ammonia, followed by high-temperature annealing. The detailed synthesis procedure was reported previously.2 The as-prepared BNNSs possess diameters of hundreds of nanometres. To investigate DNA absorption of BNNSs, a DNA sodium salt (DNA SS) was used to interact with BNNSs. Transmission electron microscopy (TEM) was used to study the morphology of DNA SS loaded BNNSs (DNA SS-BNNSs). It was revealed that some amorphous materials were coated on the surface of BNNSs after interacting with DNA SS (Fig. 1). The distribution of DNA SS is not uniform: it is enriched in some areas. It is suggested that DNA SS is bonded on BNNSs via electrostatic interactions between the electron-rich atoms of DNA (such as O and N) and the electrodeficient boron atoms, as well as the defective sites of BNNSs.

Thermogravimetric analysis (TGA) was used to investigate the DNA SS loading capacity of BNNSs. BN phase possesses superb structural stability and anti-oxidation ability, almost no weight loss can be observed in air up to 700℃.[23,24] Moreover, the shape of the TGA spectrum of DNA SS-BNNSs is very similar to pure DNA SS, which also indicates that the weight loss of DNA SS-BNNSs is mainly caused by DNASS other than BNNSs. A weight loss of 5.4% was obtained for DNA SS-BNNSs, as shown in Fig. 2(a). Considering that elements, such as P, Na, etc., inDNASS will be transferred to

oxides, the actual DNA SS portion loaded on BNNSs is estimated to be around 7 wt%. Subsequently, the releasing behavior of DNA SS-BNNSs in phosphate-buffered saline (PBS) solution was investigated. Since it was found that BNNSs tend to locate inside lysosome compartments of cells and the pH in lysosome is around 5.0, a PBS solution with pH .5 was used. The releasing profile of DNA SSBNNSs is shown in Fig. 2(b). It was revealed that DNA SS quickly released in the first 12 h, and the release became much slower in the following stage. A sustained releasing property was demonstrated. The kinetics is useful for cases that require a high initial dose followed by a more stable release of smaller doses.

To investigate cell uptake and trafficking of BNNSs, 293XL-TLR9 cells were incubated with rhodamine B isothiocyanate (RBITC)- loaded BNNSs. The fluorescence confocal microscopy images are shown in Fig. 3(a). From the differential interference contrast (DIC) and overlay images, red-emitting BNNSs were found to be accumulated inside the cells. The horizontal section showed that the BNNSs locate around the nucleus (Fig. 3(a)). Further doublestaining analysis with lysosomal-associated membrane protein 1 (LAMP1) revealed that BNNSs locate inside lysosome compartments of the cells (Fig. 3(b)). Cells after internalization of RBITClabeled BNNSs were incubated for a long time. After 72 hours, a mean distribution of red fluorescence from BNNSs was obtained (Fig. 3(c)) indicating that the cells still maintain the BNNSs after proliferation. Keeping in mind the interaction between DNA SS and BNNSs, these results suggest that BNNSs have the potential to be used as novel carriers for DNAs, proteins and drugs into lysosome compartments of cells.

Now we will demonstrate that BNNSs can be used to deliver CpG ODN into cells and activate TLR9 that is originally localized in the endoplasmic reticulum (ER) and transferred to the lysosome for the binding to CpG ODN. As the first step, uptake of CpG ODNloaded BNNSs into 293XL-TLR9 cells was investigated using 3'-fluorescein isothiocyanate (FITC)-labeled CpG ODN loaded BNNSs. DIC images revealed that pristine BNNSs, free FITC-labeled CpG ODN and FITC-labeled CpG ODN loaded BNNSs had no significant effects on cellular morphology. In addition, as shown in Fig. 4(a), fluorescence was not observed from the cells incubated together with FITC-labeled CpG ODN due to the low efficiency of uptake, while FITC-labeled CpGODNloadedBNNSs were peculiarly internalized by the cells. This indicates that BNNSs act as efficient and stable carriers for CpG ODN transfection into cells.

CpG ODN loaded BNNSs were found to activate TLR9. TLR9 activation follows a common pathway involving the transcription factor NF-kB, which is translocated to the nucleus for direct upregulation of cytokine/chemokine gene expression. Therefore, the relative NF-kB activity in

TLR9-expressing cells was determined as an index of TLR9 activation.25 Free FTIC-labeled CpG ODNs and pristine BNNSs were used as control samples. As shown in Fig. 4(b), not surprisingly, the BNNSs and free CpG ODNs did not show any effects on TLR9 activation, while FITC-labeled CpG ODN loaded BNNSs exhibited significantly higher NF-kB activity. It is clearly demonstrated that BNNSs increased the immunostimulatory activity of CpG ODN, which may result from the increase of uptake of CpG ODN to the lysosome.

Conclusions

In summary, we demonstrated that BNNSs possess decent biocompatibility and can be used as carriers for bio-molecules. The interactions between DNA and BNNSs were firstly studied, which indicates that BNNSs can be loaded with DNA and DNA can be released at controlled conditions. Cell incubation experiments indicate that BNNSs can be easily taken into cells and uptake of BNNSs does not affect cell proliferation. Subsequently, BNNSs were used as a carrier for CpG ODN and TLR9 was activated successfully by CpG ODN loaded BNNSs. Keeping in mind the superb structural stability, favorable morphology and decent biocompatibility of BNNSs, our results strongly supported that BNNSs can be used as a suitable carrier for CpG ODN, which is critically important for development of therapy for various allergy therapeutics and cancers.

Notes and references

1 N. G. Chopra, R. J. Luyken, K. Cherrey, V. H. Crespi, M. L. Cohen, S. G. Louie and A. Zettl, Science, 1995, 269, 966.

2 C. C. Tang, Y. Bando, Y. Huang, C. Y. Zhi and D. Golberg, Adv. Funct. Mater., 2008, 18, 3653.

3 O. R. Lourie, C. R. Jones, B. M. Bartlett, P. C. Gibbons, R. S. Ruoff and W. E. Buhro, Chem. Mater., 2000, 12, 1808.

4 D. Pacil_e, J. C. Meyer, C. € O. Girit and A. Zettl, Appl. Phys. Lett., 2008, 92, 133107.

5 W. Q. Han, L. Wu, Y. Zhu, K. J. Watanabe and T. Taniguchi, Appl. Phys. Lett., 2008, 93, 223103.

6 C. Y. Zhi, Y. Bando, C. Tang, H. Kuwahara and D. Golberg, Adv. Mater., 2009, 21, 2889.

7 C. Y. Zhi, Y. Bando, C. C. Tang and D. Golberg, Mater. Sci. Eng., R, 2010, 70, 92.

8 W. L. Wang, Y. Bando, C. Zhi, W. Fu, E. G. Wang and D. Golberg, J. Am. Chem. Soc., 2008, 190, 8144.

9 X. Chen, P. Wu, M. Rousseas, D. Okawa, Z. Gartner, A. Zettl and C. R. Bertozzi, J. Am. Chem. Soc., 2009, 131, 890.

10 E. Jonsson, L. Simonsen, M. Karlsson and R. Larsson, Ann. Oncol., 1998, 9, 172.

11 R. S. Waritz, B. Ballantyne and J. J. Clary, J. Appl. Toxicol., 1998, 18, 215.

12 H. Hemmi, O. Takeuchi, T. Kawai, T. Kaisho, S. Sato, H. Sanjo, M. Matsumoto, K. Hoshino, H. Wagner, K. Takeda and S. Akira, Nature, 2000, 408, 740.

13 S. Bauer, C. J. Kirschning, H. Hacker, V. Redecke, S. Hausmann, S. Akira and G. B. Lipford, Proc. Natl. Acad. Sci. U. S. A., 2001, 98, 9237.

14 H. Hacker, R. M. Vabulas, O. Takeuchi, O. Hoshino, S. Akira and H. Wagner, J. Exp. Med., 2000, 192, 595.

15 F. Shi and D. J. Hoekstra, J. Controlled Release, 2004, 97, 189.

16 H. Bartz, Y. Mendoza, M. Gebker, M. Fischborn, K. Heeg and A. Dalpke, Vaccine, 2004, 23, 148.

17 T. H. Chuang, J. Lee, L. Kline, J. C. Mathison and R. J. Ulevitch, J. Leukocyte Biol., 2002, 71, 538.

18 J. P. Sheehan and H. C. Lan, Blood, 1998, 92, 1617.

19 V. Sokolova, T. Knuschke, A. Kovtun, J. Buer, M. Epple and A. M. Westendorf, Biomaterials, 2010, 31, 5627.

20 M. I. Shukoor, F. Natalio, M. N. Tahir, M. Wiens, M. Tarantola, H. A. Therese, M. Barz, S. Weber, M. Terekhov, H. C. Schroder, W. E. G. Muller, A. Janshoff, P. Theato, R. Zentel, L. M. Schreiber and W. Tremel, Adv. Funct. Mater., 2009, 19, 3717.

21 K. D. Wilson, S. D. de Jong and Y. K. Tam, Adv. Drug Delivery Rev., 2009, 61, 233.

22 P. Malyala, D. T. O'Hagan and M. Singh, Adv. Drug Delivery Rev., 2009, 61, 218.
23 D. Golberg, Y. Bando, K. Kurashima and T. Sato, Scr. Mater., 2001, 44, 1561.
24 Y. Chen, J. Zou, S. J. Campbell and G. Le Caer, Appl. Phys. Lett., 2004, 84, 2430.
25 T. H. Chuang, J. Lee, L. Kline, J. C. Mathison and R. J. Ulevitch, J. Leukocyte Biol., 2002, 71, 538.

Figure legends

Fig. 1 TEM images of DNA SS-BNNSs. In (a), the blue arrow indicates a layer of DNA SS on BNNSs.

Fig. 2 (a) TGA analysis of DNA SS-BNNSs. A weight loss of 5.4% was revealed and theDNASS loading capacity of BNNSs was estimated to be around 7%. (b) Releasing profile of DNA SS-BNNSs.

Fig. 3 Cellular uptake of BNNS particles. (a) Cells were stained with DAPI and incubated with RBITC-labeled BNNSs. The merged images show cell uptake of BNNSs. (b) Cells with lysosome stained with LAMP1 were incubated with RBITC-labeled BNNSs. The merged images show that BNNSs locate in lysosome. (c) Distribution of BNNS during proliferation. Cells were incubated with RBITC-labeled BNNS for 24, 48 and 72 hours respectively. Cells were stained with DAPI before microscopic analysis.

Fig. 4 Cell uptake of FITC-labeled CpG ODN loaded BNNSs, pristine BNNSs and free FITC-labeled CpG ODNs, as well as the effects of the FITC-labeled CpG ODN loaded BNNSs for TLR9 activation. (a) Confocal microscopy of DIC, fluorescence and merge images of 293XLhTLR9 cells. (b) NF-kB activation efficiency of FITC-labeled CpG ODN-loaded BNNSs compared with free FITC-labeled CpG ODNs and pristine BNNSs in 293XL-hTLR9 cells.

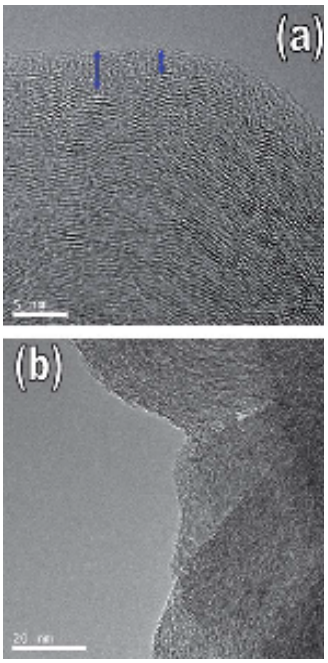

Fig. 1 TEM images of DNA SS-BNNSs. In (a), the blue arrow indicates a layer of DNA SS on BNNSs.

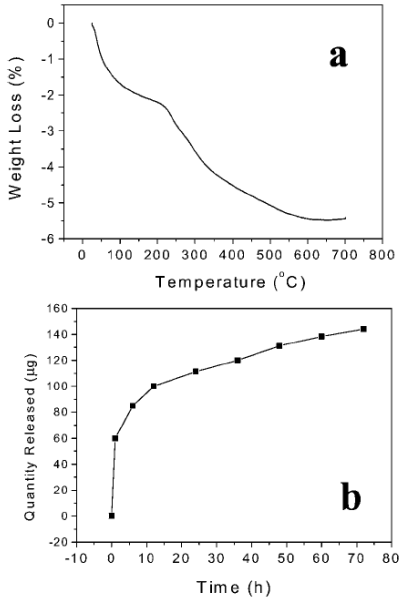

Fig. 2 (a) TGA analysis of DNA SS-BNNSs. A weight loss of 5.4% was revealed and theDNASS loading capacity of BNNSs was estimated to be around 7%. (b) Releasing profile of DNA SS-BNNSs.

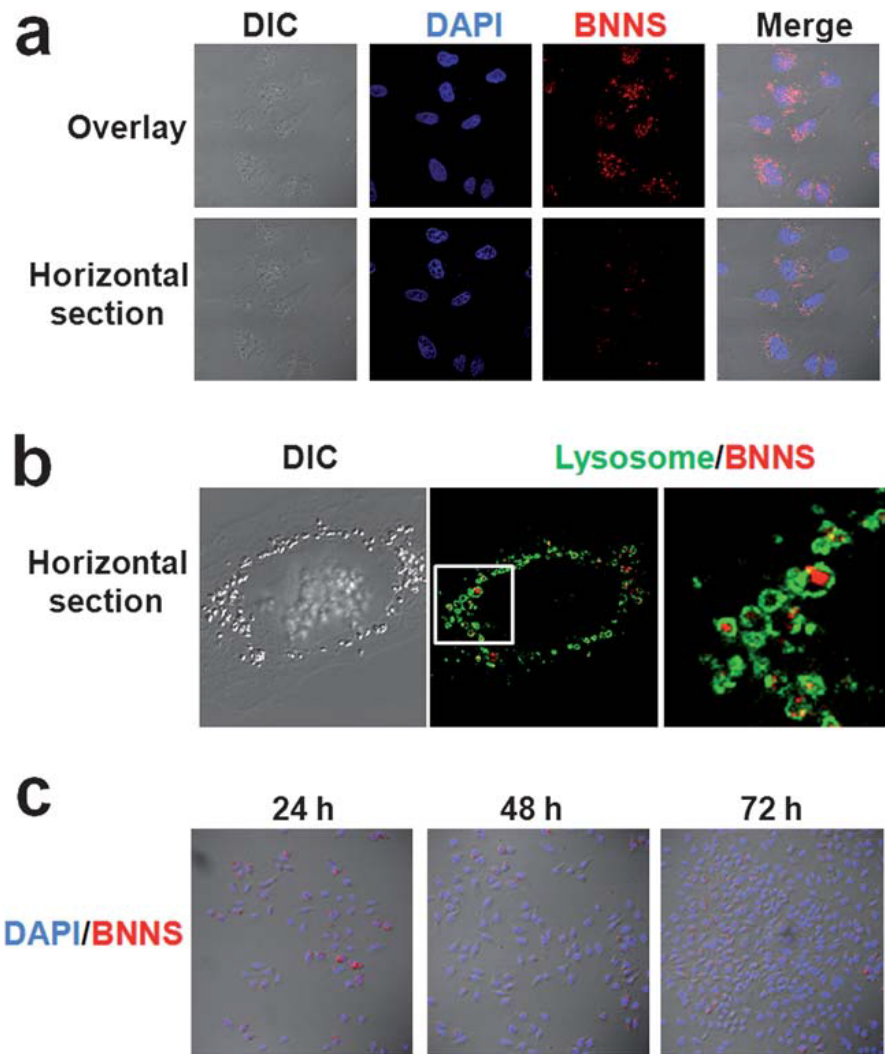

Fig. 3 Cellular uptake of BNNS particles. (a) Cells were stained with DAPI and incubated with RBITC-labeled BNNSs. The merged images show cell uptake of BNNSs. (b) Cells with lysosome stained with LAMP1 were incubated with RBITC-labeled BNNSs. The merged images show that BNNSs locate in lysosome. (c) Distribution of BNNS during proliferation. Cells were incubated with RBITC-labeled BNNS for 24, 48 and 72 hours respectively. Cells were stained with DAPI before microscopic analysis.

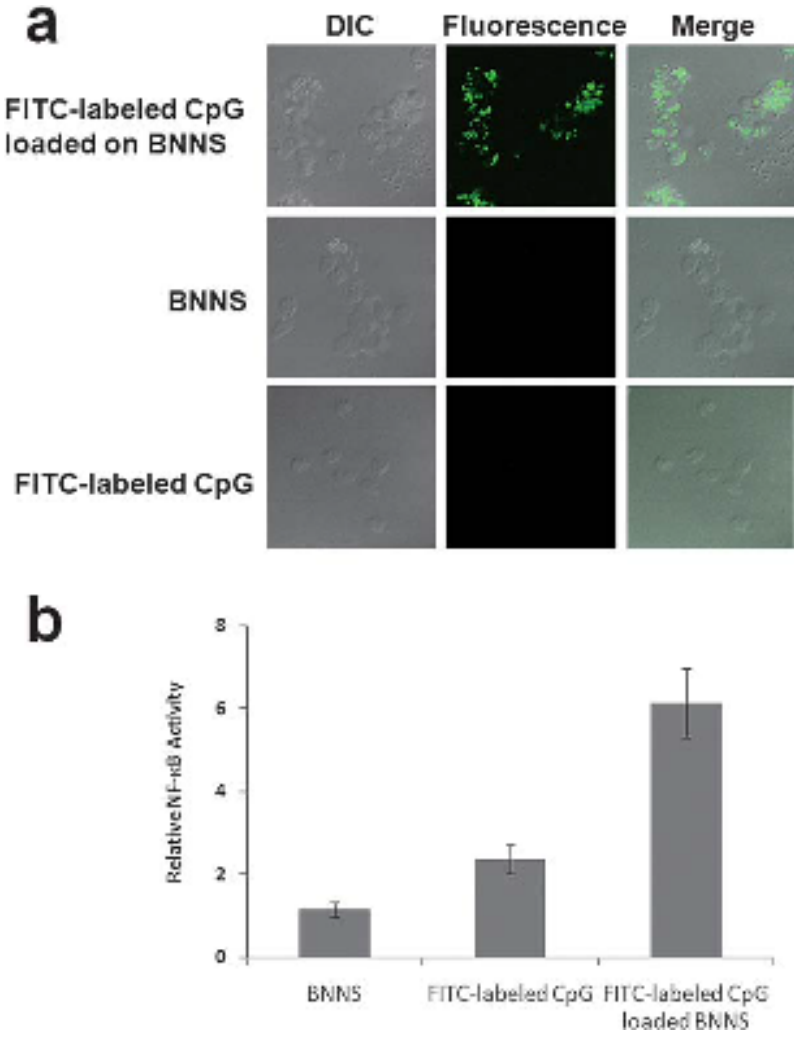

Fig. 4 Cell uptake of FITC-labeled CpG ODN loaded BNNSs, pristine BNNSs and free FITC-labeled CpG ODNs, as well as the effects of the FITC-labeled CpG ODN loaded BNNSs for TLR9 activation. (a) Confocal microscopy of DIC, fluorescence and merge images of 293XLhTLR9 cells. (b) NF-kB activation efficiency of FITC-labeled CpG ODN-loaded BNNSs compared with free FITC-labeled CpG ODNs and pristine BNNSs in 293XL-hTLR9 cells.

BN nanospheres as CpG ODN carrier for activation of toll-like receptor 9

Chunyi Zhi[*a], Wenjun Meng[b,c], Tomohiko Yamazaki[b,c], Yoshio Bando[a], Dmitri Golberg[a], Chengchun Tang[a], Nobutaka Hanagata[*b,c,d]

[a]*International Center for Materials Nanoarchitectonics (MANA), National Institute for Materials Science (NIMS),*
Namiki 1-1, Tsukuba, Ibaraki 305-0044, Japan
[b]*Graduate School of Life Science, Hokkaido University*
N10W8, Kita-ku, Sapporo 060-0812, Japan.
[c]*Biomaterials Center, National Institute for Materials Science (NIMS),*
1-2-1 Sengen, Tsukuba, Ibaraki 305-0047, Japan.
[d]*Nanotechnology Innovation Center, National Institute for Materials Science (NIMS),*
1-2-1 Sengen, Tsukuba, Ibaraki 305-0047, Japan.
E-mail addresses: ZHI.chunyi@nims.go.jp; HANAGATA.Nobutaka@nims.go.jp

Supporting Information

1. Materials and Methods

Preparation of BN nanospheres

A traditional tube style CVD system was used to synthesize BN nanospheres. B(OMe)3 and NH3 were loaded into the furnace. The exhausting gas that contained ammonia was fed through a water or acid solution bath to collect the remnant toxic gas. Thus, the CVD system was kept under a positive pressure. Growth temperature was kept at 950 °C. A product was collected from the downstream side slightly away from the furnace center. The collected product was further annealed under protection of ammonia at 1375 °C.

DNA sodium salt loading and releasing of BN nanospheres

For loading DNA sodium salt on BN nanospheres, 200 mg DNA sodium salt (Deoxyribonucleic Acid sodium salt from salmon spermary produced by Wako company) was added to pure water and the solution was heated up to 90□ and stirred for 1h. Then 500 mg pristine BN nanospheres were mixed, followed by 24h stirring. Finally, BN nanospheres were centrifuged out, washed and dried. For releasing, a 20 mg DNA sodium salt loaded BN nanospheres hybrid was added to

phosphate-buffered saline solution (PBS, 20 ml, PH 5.0), and stirred at 150 rpm at room temperature. At certain time intervals, aliquots of PBS (4 ml) were taken out by centrifugation to test the concentration of released DNA sodium salt, and 4 ml fresh PBS was added to the solution of DNA sodium salt loaded BNNSs.

Cell cultures

293XL-hTLR9 cells stably expressing human TLR9 were purchased from "Invivogen" Company (California, US). Cells were grown in DMEM medium supplemented with 10 (v/v) % FBS, 50 units/ml penicillin, 50 mg/ml streptomycin, 100 μg/mL normocin and 10 μg/mL blasticidin at 37 °C in humidified air containing 5% CO2. Cells were seeded on 24-well culture plates for transfection and stimulation experiments.

Unmethylated cytosine-phosphate-guanine (CpG) oligodeoxynucleotide(ODN)

3'-Fluorescein isothiocyanate (FITC) labeled natural phosphorodiester CpG ODN 2006 was purchased from "Fasmac" Company (Kanagawa, Japan). The sequence of CpG ODN 2006 is 5'-TCGTCGTTTTGTCGTTTTGTCGTT-3'. The CpG ODN was diluted in sterilized water and stored at -20°C before use.

Preparation of FITC-labeled CpG ODN loaded BNNSs

BNNSs solution and 3'-FITC-labeled CpG ODN solution were mixed in PBS buffer and continuously shaken at 4 °C for 4 h. In a typical experiment, 40 μL of BNNSs solution (1mg/mL in PBS) and 6 μL of FITC-labeled CpG ODN solution (100 μM stock in sterilized water) were mixed by rotation for 4 h.

Cellular uptake of BNNSs

Rhodamine B isothiocyanate (RBITC)-loaded BNNSs were used to investigate the cellular uptake and localization of BNNSs into the cells. 1x105 293XL-TLR9 cells were seeded in a 35mm perti dish with glass bottom and pre-incubated at 37 °C in humidified air containing 5% CO2 for 48 h. Subsequently, RBITC-loaded BNNSs were added to the petri dishes at a final concentration of 10 ng/ml. Cells were fixed with 4 (v/v) % paraformaldehyde after culture and in some cases stained with DAPI and antibody. Lysosome staining was achieved by incubation the cells with Rabbit polyclonal to LAMP1 (abcam, Cambridge, UK) and then Alexa Fluor 488 goat anti-rabbit IgG (H+L) secondary antibody (invitrogen, Calfornia, US). Free BNNSs, FITC-labeled CpG and FITC-labeled CpG loaded BNNSs were used in a parallel manner for analysis of CpG uptake into cells

NF-κB luciferase assay

For monitoring transient NF-κB activation, 293XL-hTLR9 cells were seeded into 24-well plates at a

density of approximately 1.5x105 cells per well and transiently transfected with pNiFty-luc (a TLR9-signaling reporter plasmid, purchased from Invivogen) and pGL4.74 (a CMV promoter -Renilla luciferase gene contained plasmid, as an internal control for variations in transfection efficiency, purchased from Promega (Wisconsin, US)) using transfection reagent, LyoVec (Invivogen). After a 24-hour culture, cells were stimulated with 0.3 μM of FITC-labeled CpG, free BNNSs, or FITC-labeled CpG loaded BNNSs respectively for another 24 hours. The luciferase activities were evaluated using the Dual-Luciferase assay system (Promega). Stimulated cells were lysed using a passive lysis buffer, and the resulting lysates were assayed for relative luciferase activity using a TD-20/20 luminometer (Promega) according to the manufacturer's instructions. The data were shown as fold increase in NF-κB activity over the medium control.

Others

The microstructures were analyzed using a JEOL-3000F high-resolution field-emission transmission electron microscope operated at 300 kV. The differential interference contrast (DIC) and confocal fluorescence images were acquired by an SP5 confocal fluorescence microscope (CLSM; Leica microsystems, Germany).

Figure S1. TEM images of BN nanospheres.

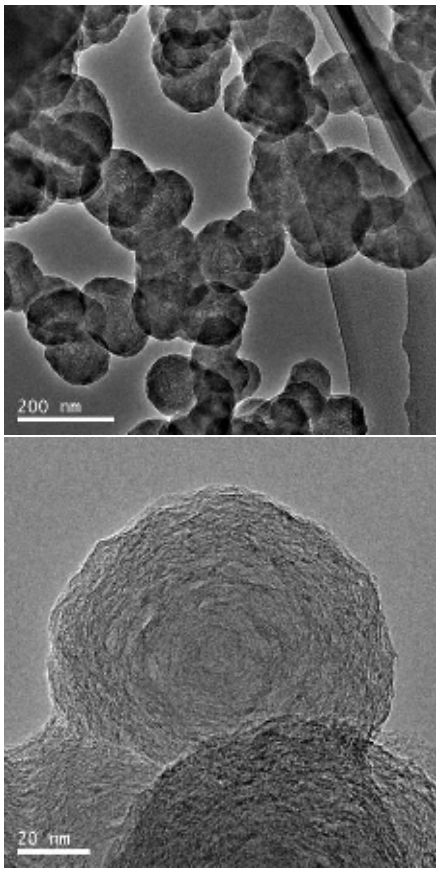

Figure S2. TGA analysis of a DNA sodium salt and a BN nanospheres-DNA sodium salt hybrid. The weight loss behavior of BN nanospheres-DNA sodium salt hybrid is very close to that of pure DNA sodium salt, which indicates that the weight loss is mainly due to oxidation of DNA sodium salt rather than BN nanospheres. In addition, DNA sodium salt itself has a final weight loss of 73%.